J. Phase Equilib. Diffus. (2024) 45:447–458
https://doi.org/10.1007/s11669-024-01095-x

ORIGINAL RESEARCH ARTICLE

Phase Equilibria and Thermodynamic Properties of Selected Compounds in the Ag-Ga-Te-AgBr System

Mykola Moroz[1] · Fiseha Tesfaye[2] · Pavlo Demchenko[3] · Myroslava Prokhorenko[4] · Emanuela Mastronardo[5] · Oleksandr Reshetnyak[6] · Daniel Lindberg[7] · Leena Hupa[2]

Submitted: 29 September 2023 / in revised form: 20 January 2024 / Accepted: 31 January 2024 / Published online: 23 February 2024

Abstract The equilibrium $T - x$ space of the Ag-Ga-Te-AgBr system in the part Ag_2Te-GaTe-Te-AgBr-Ag_2Te below 600 K has been divided into separate phase regions using the electromotive force (EMF) method. Accurate experimental data were obtained using the following electrochemical cells (ECs): (−) IE | NE | SSE | R{Ag^+} | PE | IE (+), where IE is the inert electrode (graphite powder), NE is the negative electrode (silver powder), SSE is the solid-state electrolyte (glassy Ag_3GeS_3Br), PE is the positive electrode, R{Ag^+} is the region of PE that is contact in with SSE. At the stage of cell preparation, PE is a non-equilibrium phase mixture of the well-mixed powdered compounds Ag_2Te, GaTe, Ga_2Te_3, AgBr, and tellurium, taken in ratios corresponding to two or three different points of interest for each of the phase regions. The equilibrium set of phases was formed in the R{Ag^+} region at 600 K for 48 h with the participation of the Ag^+ ions. Silver cations, displaced for thermodynamic reasons from the NE to the PE of ECs, acted as catalysts, i.e., small nucleation centers of equilibrium phases. The spatial position of the established phase regions relative to the position of silver was used to express the overall reactions of synthesis of the binary Ga_2Te_5, Ga_7Te_{10}, Ga_3Te_4, ternary $AgGa_5Te_8$, and quaternary $Ag_3Ga_{10}Te_{16}Br$, $Ag_3Ga_2Te_4Br$, $Ag_{27}Ga_2Te_{12}Br_9$ compounds in the PE of ECs. The values of the standard thermodynamic functions (Gibbs energies, enthalpies, and entropies) of these compounds were determined based on the temperature dependencies of the EMF of the ECs.

Keywords EMF method · Gibbs energy · phase equilibria · thermoelectric materials · thermodynamic properties

This invited article is part of a special tribute issue of the *Journal of Phase Equilibria and Diffusion* dedicated to the memory of Thaddeus B. "Ted" Massalski. The issue was organized by David E. Laughlin, Carnegie Mellon University; John H. Perepezko, University of Wisconsin–Madison; Wei Xiong, University of Pittsburgh; and *JPED* Editor-in-Chief Ursula Kattner, National Institute of Standards and Technology (NIST).

✉ Mykola Moroz
m.v.moroz@nuwm.edu.ua

[1] Department of Chemistry and Physics, National University of Water and Environmental Engineering, Rivne 33028, Ukraine

[2] Johan Gadolin Process Chemistry Centre, Åbo Akademi University, 20500 Turku, Finland

[3] Department of Inorganic Chemistry, Ivan Franko National University of Lviv, Lviv 79005, Ukraine

[4] Department of Cartography and Geospatial Modeling, Lviv Polytechnic National University, Lviv 79013, Ukraine

[5] Department of Engineering, University of Messina, 98166 Messina, Italy

[6] Department of Physical and Colloid Chemistry, Ivan Franko National University of Lviv, Lviv 79005, Ukraine

[7] Department of Chemical and Metallurgical Engineering, Aalto University, 02150 Espoo, Finland

1 Introduction

Over the past few decades, silver-containing chalcogenides and chalcohalides have attracted significant attention among scientists and engineers due to their potentially environmentally sound application in solid-state ionics, and nonlinear optical devices, photovoltaic absorbers, as well as thermoelectric materials (TMs).[1-6] Moreover, multinary chalcogenides and chalcohalides have been considered

interesting scientific objects due to the diversity of their crystal structures and physicochemical properties.[7-12]

The TMs offer various opportunities in power generation by directly converting waste heat to electricity. Moreover, TMs devices are quiet in operation, do not release emissions, and are components of environmentally friendly technologies.[13-15] The typical binary TMs based on bismuth and lead tellurides have a narrow application due to their low efficiency and environmental reasons.[16,17] The criterion for choosing compounds for application in the thermoelectric devices is a dimensionless thermoelectric figure of merit parameter $ZT = (S^2\sigma)T/k$ (where S is the Seebeck coefficient, σ is the electrical conductivity, k is the thermal conductivity, and T is the absolute temperature).[18] In crystals, which simultaneously have a strong covalent bond that provides high electronic conductivity, and disordered mobile ions (like a "quasi-liquid"), there is a possibility of independent optimization of both factors.[19-21] The focus on tellurium as the heaviest non-radioactive chalcogen is due to the possibility of decreasing the thermal conductivity coefficient.[22] Optimization of synthesis of new TMs is impossible without a comprehensive analysis of the thermodynamic properties of intermediate phases and construction of equilibrium phase diagrams.

According to different literature reports,[23-31] most of the binary, ternary, and quaternary compounds of the Ag-Ga-Te-AgBr system are located in the Ag_2Te-GaTe-Te-AgBr-Ag_2Te part. In particular, the GaTe-Te part consists of the following compounds Ga_3Te_4, Ga_7Te_{10}, Ga_2Te_3, and Ga_2Te_5; section Ag_2Te-Ga_2Te_3 contains Ag_9GaTe_6, $AgGaTe_2$, and $AgGa_5Te_8$; section Ag_2Te-AgBr contains Ag_3TeBr; and section AgBr-Ga_2Te_3 contains $AgGa_2Te_3Br$. According to Blachnik and Klose,[29] compounds GaTe and Ga_2Te_3 melt congruently at 1108 and 1071 K, respectively; Ga_3Te_4 is formed at 1057 K by the peritectic reaction of the melt and Ga_2Te_3; Ga_2Te_5 exists in a limited temperature range of 681-757 K. A trigonal Ga_7Te_{10} was synthesized from pure components at 1020 K.[27] To our knowledge, there is no information on the thermal and thermodynamic stability of the Ga_7Te_{10} at 300 K. Kramer et al.[24] found that Ag_9GaTe_6 melts incongruently at 978 K and underdoes a phase transition in the range of 275-303 K. The Ag_3TeBr compound is formed at 710 K by the peritectic reaction of Ag_2Te with the melt.[23] The crystal structure of the $AgGa_2Te_3Br$ compound has been indexed to the tetragonal system, space group I-4, a = 0.62977(3) nm and c = 1.19473(7) nm.[25] The ternary compounds Ag_9GaTe_6, $AgGaTe_2$, and $AgGa_5Te_8$ of the quasi-binary system Ag_2Te-Ga_2Te_3 belong to the class of thermoelectric materials.[28,30,31]

The effect of replacing part of the gallium cations of the compound p-Ag_9GaTe_6 according to the scheme $Ag_9Ga_{1-\delta}M_\delta Te_6$ (M = Cd, Zn, Mg, Nb; δ = 0.05) on the ZT values is given in (Ref 31). In the case of Cd doping, achieving the thermoelectric figure of merit parameter of $ZT \approx 0.6$ at 600 K. Such method of increasing the ZT value is ineffective in the case of a thermodynamically unbalanced state of the doping component in the crystal lattice of the compound. The action of external factors, such as changes in temperature, pressure, radiation, etc. will contribute to the migration of impurities at the grain boundary, which will lead to a decrease in the ZT value of the sample over time. It is possible to avoid a decrease in the ZT value during the operation of a doped thermocouple by producing it in the form of an equilibrium solid solution based on a quaternary compound. As an example, for doping of the Ag_9GaTe_6, $AgGaTe_2$, and $AgGa_5Te_8$, it is possible to use quaternary compounds of the Ag_2Te-Ga_2Te_3-AgBr region. This region is part of the Ag-Ga-Te-AgBr system, where the formation of quaternary compounds $Ag_3Ga_{10}Te_{16}Br$, $Ag_3Ga_2Te_4Br$, and $Ag_{27}Ga_2Te_{12}Br_9$ is possible at the intersection points of the $AgGa_5Te_8$-AgBr, $AgGaTe_2$-AgBr, Ag_9GaTe_6-AgBr composition lines with the Ga_2Te_3-Ag_3TeBr composition line. There are no previous reports on quaternary compounds of mentioned compositions. The thermodynamic conditions for the formation of quaternary phases likely correspond to the temperature values $T < 600$ K, although there are kinetic obstacles to such a process. Kinetic obstacles to the synthesis of phases from pure substances and binary compounds can be overcome with the participation of a catalyst, for example Ag^+ ions, as small nucleation centers of equilibrium phases.[32,33]

The purpose of this work was to establish the phase equilibria of the Ag-Ga-Te-AgBr system in the part Ag_2Te-GaTe-Te-AgBr-Ag_2Te below 600 K and to determine the standard thermodynamic properties of compounds by the electromotive force (EMF) method.

2 Experimental Procedure

The high-purity substances Ag (>99.9 wt.%, Alfa Aesar, Germany), Ga, Te (>99.99 wt.%, Alfa Aesar, Germany), and binary compound AgBr (>99.99 wt.%, Alfa Aesar, Germany) were used to synthesize the binary and ternary compounds. Evacuated melts of the Ag_2Te, GaTe, and Ga_2Te_3 compounds, cooled to room temperature, were crushed to a particle size of $\sim 1 \cdot 10^{-6}$ m for preparation of the positive electrodes (PE) of electrochemical cells (ECs). Melts of the Ga_7Te_{10}, $AgGaTe_2$, and $AgGa_5Te_8$ compounds cooled to a temperature of 630 K were annealed for two weeks, followed by cooling to room temperature with the furnace turned off. The phase composition of the synthesized compounds was analyzed by an x-ray diffraction (XRD) technique. The STOE STADI P diffractometer equipped with a linear position-sensitive detector PSD, in a Guinier geometry (transmission mode, Cu$K\alpha_1$ radiation, a

bent Ge(111) monochromator, and 2 θ/ω scan mode) was used for these investigations. The following software programs STOE WinXPOW,[34] PowderCell,[35] FullProf,[36] and crystal structure databases[37,38] were applied to analyze the obtained results.

The modified EMF method[39,40] was used both to establish the phase equilibria in the GaTe-$AgGa_5Te_8$-Te region below 600 K and to determine the thermodynamic parameters of compounds. For these investigations, a certain number of ECs were assembled:

$$(-)\ \text{IE} \mid \text{NE} \mid \text{SSE} \mid \text{R}\{Ag^+\} \mid \text{PE} \mid \text{IE}\ (+)$$

where IE is the inert electrode (graphite powder), NE is the negative electrode (silver powder), SSE is the solid-state electrolyte (glassy Ag_3GeS_3Br[41]), and R{Ag^+} is the region of PE that is in contact with SSE. At the stage of cell preparation, PE is the non-equilibrium phase mixture of the well-mixed powdered binary compounds Ag_2Te, GaTe, Ga_2Te_3, AgBr, and pure substance tellurium. Compositions of these mixtures covered the entire composition space of the Ag_2Te-GaTe-Te-AgBr-Ag_2Te system. An equilibrium set of phases was formed in the R{Ag^+} region at 600 K after 48 h. The Ag^+ ions, displaced for thermodynamic reasons from the NE to the PE electrodes of the ECs, acted as catalysts, i.e., small nucleation centers of equilibrium phases.[32,33]

The experiments were performed in a resistance furnace as previously described in literature.[42] To assemble the ECs, a fluoroplastic base with a hole with a diameter of 2 mm was used. The powder components of ECs were pressed at pressure 10^8 Pa into the hole under a load of (2.0 ± 0.1) tons to a density of $\rho = (0.93 \pm 0.02)\cdot\rho_0$, where ρ_0 is the experimentally determined density of cast samples. The assembled cells were placed in a quartz tube with nozzles for the purging of argon gas.[43,44] The argon gas flow had a direction from the NE to PE of ECs at the rate of (10.0 ± 0.2) $cm^3 \cdot min^{-1}$. The temperature of ECs was maintained by an electronic thermostat with $\pm$ 0.5 K accuracy. A Picotest M3500A digital voltmeter with an input impedance of $> 10^{12}$ Ohms was used to measure the EMF (E) values of the cells (accuracy $\pm$ 0.3 mV) at different temperatures. The reproducibility of the E versus T dependences of ECs in heating-cooling cycles was a criterion for completing the formation of the equilibrium set of phases in the R{Ag^+} region.

3 Results and Discussion

3.1 Phase Equilibria and Thermodynamic Properties of Selected Compounds of the Ag-Ga-Te System in the GaTe-$AgGa_5Te_8$-Te Part Below 600 K

Charoenphakdee et al.[30] reported that the $AgGa_5Te_8$ compound was obtained by cooling the melt to a temperature of 873 K and subsequent homogenization for 1 week. In our research, the $AgGa_5Te_8$ compound was not obtained by cooling the melt to 630 K followed by annealing for two weeks. The diffraction pattern of the synthesized powder sample is shown in Fig. 1.

The presence of a solid solution of Ag in Ga_2Te_3, i.e. $Ag_xGa_2Te_3$ (structure type (ST) ZnS, space group (SG) F–43 m) and a minor admixture of an unidentified phase have been established by the XRD method. The refined unit-cell parameter a = 0.59786(5) nm is greater than $a \sim$ (0.587-0.590) nm for Ga_2Te_3[37,38] (JCPDS cards No. 35-1490, 79-2443, 89-7202), thus indicating the formation of a solid solution.

A metastable, for kinetic reasons, combination of the mentioned phases was confirmed by an attempt to implement the reaction $AgGaTe_2 + 2Ga_2Te_3 = AgGa_5Te_8$. For this reason, a well-mixed blend of the $AgGaTe_2$ and $2Ga_2Te_3$ compounds was evacuated, kept for two weeks at

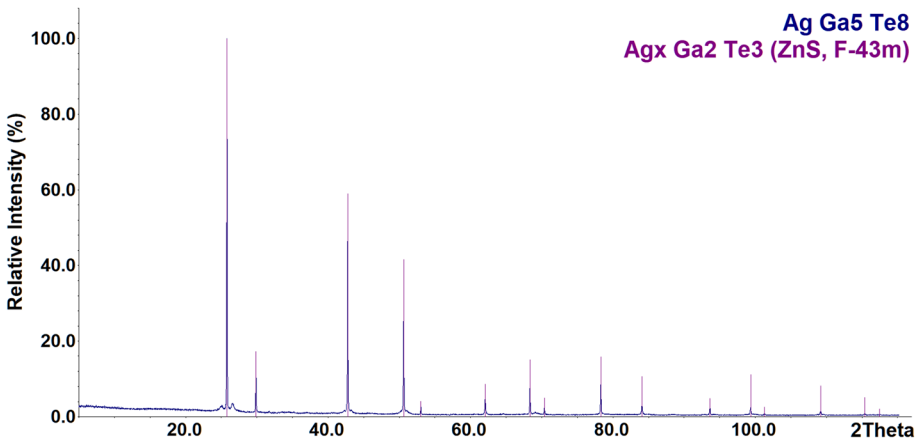

Fig. 1. X-ray powder diffraction pattern of the sample with nominal composition $AgGa_5Te_8$, obtained by cooling the melt to 630 K. Detected composition of the sample and identified phase (with structure type and space group indicated) are shown in the upper right corner

630 K, and cooled to room temperature. According to the XRD results presented in Fig. 2, the orthorhombic $AgGa_5Te_8$ compound was also not obtained. The sample contained characteristic peaks of the phases $Ag_xGa_2Te_3$ (ST ZnS, SG *F*–43*m*), $AgGaTe_2$ (ST $CuFeS_2$, SG *I*–42*d*), and pure Te (ST Se, SG $P3_121$)[37] (JCPDS Cards No. 45-1278, 75-0116, 80-2200, 65-2748, 36-1452). Thus, results of the XRD have shown that the orthorhombic $AgGa_5Te_8$ compound decomposes at a certain value of the temperature in the range of 630-873 K.

The XRD pattern of a sample with a nominal composition Ga_7Te_{10}, synthesized at 1020 K followed by annealing at 630 K for 2 weeks is shown in Fig. 3. The main phase Ga_2Te_3 (ST ZnS, SG *F*-43*m*, refined unit-cell parameter $a = 0.5897(7)$ nm) and the additional phase Ga_7Te_{10} with rhombohedral structure were identified[37] (JCPDS Cards No. 35-1490, 79-2443, 89-7202, 85-0007). Hence, the Ga_2Te_3 phase is a decomposition product of the high-temperature modification of the Ga_7Te_{10} phase.

Thus, from the analysis of the XRD patterns Fig. 1, 2 it follows that the stable at 873 K compound $AgGa_5Te_8$, decomposes at a certain value of the temperature in the range of 630-873 K. However, in this work, the existence of the $AgGa_5Te_8$ compound below 600 K was established. The existence of a low-temperature modification of $AgGa_5Te_8$ is based on the results of division of the composition space of the GaTe-$AgGa_5Te_8$-Te system by the EMF method (Fig. 4), calculations the values of thermodynamic functions of binary and ternary compounds with their further use in studies of the properties of quaternary phases. Other examples of the existence of silver-based ternary and quaternary compounds in two temperature ranges are described in elsewhere literature.[45-47]

The division of the composition space of the Ag-Ga-Te system in the GaTe-$AgGa_5Te_8$-Te part below 600 K into separate three-phase regions was carried out on the basic rules of the EMF method:[48-50]

1) within a specific phase region, the EMF value of the cell does not depend on the composition of the PE;
2) ECs with PE of different phase regions are characterized by different EMF values at $T = \text{const}$ (see Table 1 and Fig. 4);

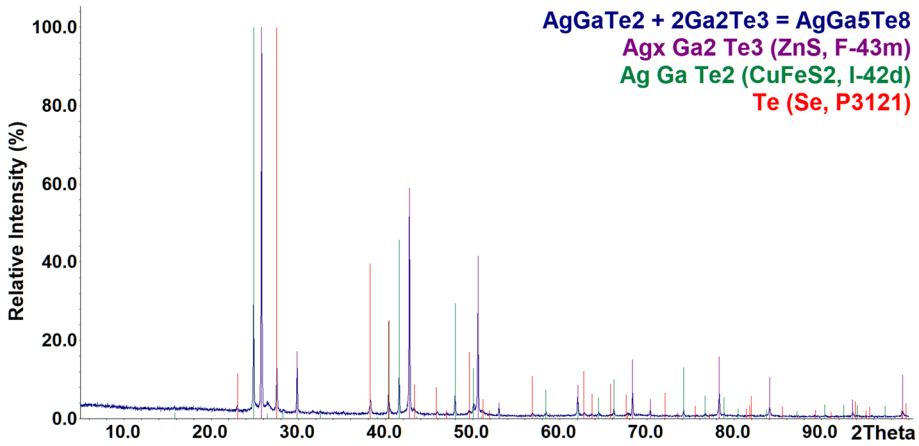

Fig. 2. X-ray powder diffraction pattern of the sample with nominal composition $AgGa_5Te_8$, obtained by solid-state synthesis mixture of the $AgGaTe_2$ and $2Ga_2Te_3$ compounds. Detected compositions of the sample and identified phases (with structure type and space group indicated) are shown in the upper right corner

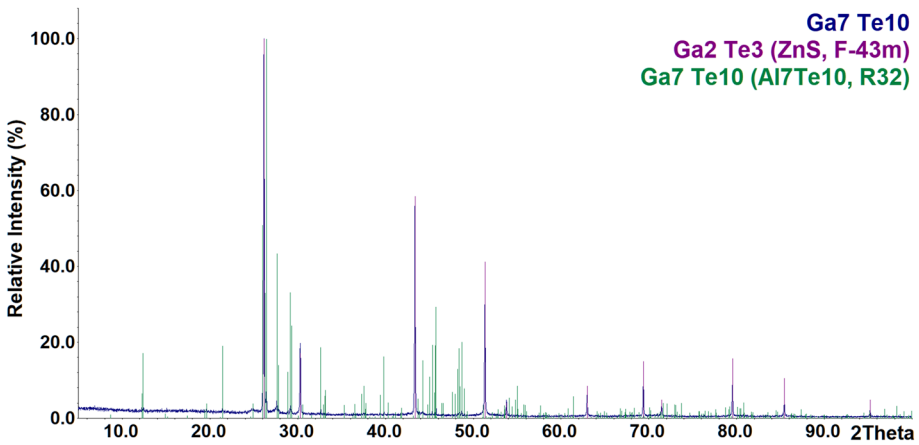

Fig. 3. X-ray powder diffraction pattern of the sample with nominal composition Ga_7Te_{10}. Compositions of the sample and identified phases (with structure type and space group indicated) are shown in the upper right corner

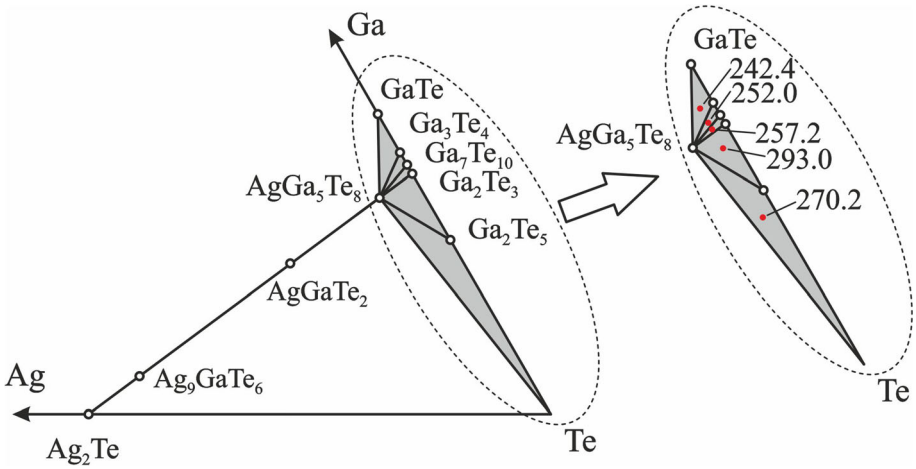

Fig. 4. Division of the composition space of the GaTe-$AgGa_5Te_8$-Te system at $T < 600$ K. Red dots indicate compositions of the PE of ECs and EMF (mV) values of the ECs at 400.4 K

Table 1 Measured values of temperature (T) and EMF (E) of the ECs with PE of different phase regions at pressure $P = 10^5$ Pa

T/K	Phase regions		T/K	Phase regions	
	(I) E/mV	(II) E/mV		(III) E/mV	(IV) E/mV
400.4	270.2	293.0	350.3	251.5	246.8
405.4	271.0	293.5	355.3	252.0	247.3
410.4	271.7	294.1	360.3	252.7	247.8
415.4	272.4	294.7	365.4	253.3	248.4
420.3	273.2	295.2	370.4	254.0	249.0
425.3	274.0	295.9	375.4	254.6	249.5
430.3	274.7	296.5	380.4	255.2	250.0
435.2	275.5	297.2	385.4	255.8	250.5
440.2	276.2	297.7	390.4	256.3	251.0
445.2	277.1	298.3	395.4	256.8	251.5
450.1	277.7	298.7	400.4	257.2	252.0
455.1	278.5	299.3	405.4	257.7	252.5

Standard uncertainties u are $u(T) = 0.5$ K, $u(P) = 10^4$ Pa, and $u(E) = 0.3$ mV.

3) the three-phase region further away from the figurative point of Ag is characterized by a higher EMF value at a specific temperature.

The spatial position of three-phase regions Ga_2Te_5-$AgGa_5Te_8$-Te (I), Ga_2Te_3-$AgGa_5Te_8$-Ga_2Te_5 (II), Ga_7Te_{10}-$AgGa_5Te_8$-Ga_2Te_3 (III), and Ga_3Te_4-$AgGa_5Te_8$-Ga_7Te_{10} (IV) relative to the silver point was used to establish the overall potential-determining reactions:

$$2Ag + 5Ga_2Te_5 = 2AgGa_5Te_8 + 9Te, \quad \text{(Eq R1)}$$

$$4Ag + 9Ga_2Te_3 + Ga_2Te_5 = 4AgGa_5Te_8, \quad \text{(Eq R2)}$$

$$Ag + 6Ga_2Te_3 = AgGa_5Te_8 + Ga_7Te_{10}, \quad \text{(Eq R3)}$$

$$Ag + 2Ga_7Te_{10} = AgGa_5Te_8 + 3Ga_3Te_4. \quad \text{(Eq R4)}$$

Reactions (R1)-(R4) took place in the PE of ECs, the phase mixtures correspond to phase regions (I)-(IV), respectively. The binary and ternary compounds in reactions (R1)-(R4) are written assuming that the phases have constant composition, which was confirmed by further calculations of thermodynamic functions of quaternary compounds (see Section 3.2). According to reactions (R1)-(R4), the ratios of binary compounds and pure tellurium for assembling the PE of ECs were established. In particular, the compounds $AgGa_5Te_8$, Ga_2Te_5, Ga_7Te_{10}, and Ga_3Te_4 are present in the PE with the following ratios of mixtures of the binary compounds and the pure substance Te: $0.5Ag_2Te + 2.5Ga_2Te_3$, $Ga_2Te_3 + 2Te$, $GaTe + 3Ga_2Te_3$, and $GaTe + Ga_2Te_3$, respectively.

The E versus T relations were obtained by the least squares method[51,52] and are presented in the form of Eq 1:

$$E = a + bT \pm k_{St}\sqrt{\left(\frac{u_E^2}{n} + u_b^2\left(T - \overline{T}\right)^2\right)}, \quad \text{(Eq 1)}$$

where a and b are coefficients of linear equation, k_{St} is the Student's parameter,[53] n is the number of experimental pairs E_i and T_i, u_E^2 and u_b^2 are the statistical dispersions of the E and b quantities, respectively.

Listed in Table 1 are the experimental values of E and T that were used to calculate the coefficients and statistical dispersions of Eq 1 in the phase regions (I)-(IV). The results of the calculations are listed in Table 2.

The Gibbs energies ($\Delta_r G$), enthalpies ($\Delta_r H$), and entropies ($\Delta_r S$) of the reactions (R1)-(R4) were calculated by the following thermodynamic equations:

$$\Delta_r G = -n\mathrm{F}E, \quad \text{(Eq 2)}$$

$$\Delta_r H = -n\mathrm{F}\left[E - \left(\frac{dE}{dT}\right)T\right], \quad \text{(Eq 3)}$$

$$\Delta_r S = n\mathrm{F}(dE/dT). \quad \text{(Eq 4)}$$

Table 2 The coefficients and statistical dispersions of E versus T dependencies of the ECs

Phase regions	$E = a + bT \pm k_{St}\sqrt{\left(\frac{u_E^2}{n} + u_b^2(T-\overline{T})^2\right)}$
(I)	$E = 209.34 + 151.97 \times 10^{-3}T \pm 2.179\sqrt{\left(\frac{2.37\times10^{-3}}{12} + 6.72 \times 10^{-7}(T-427.78)^2\right)}$
(II)	$E = 245.88 + 117.57 \times 10^{-3}T \pm 2.179\sqrt{\left(\frac{6.63\times10^{-3}}{12} + 1.88 \times 10^{-6}(T-427.78)^2\right)}$
(III)	$E = 211.32 + 114.97 \times 10^{-3}T \pm 2.179\sqrt{\left(\frac{2.00\times10^{-2}}{12} + 5.56 \times 10^{-6}(T-377.88)^2\right)}$
(IV)	$E = 210.42 + 103.93 \times 10^{-3}T \pm 2.179\sqrt{\left(\frac{2.54\times10^{-3}}{12} + 7.07 \times 10^{-7}(T-377.88)^2\right)}$

where n is the number of electrons involved in the reactions (R1)-(R4), F is the Faraday's constant, and E is the EMF of the ECs.

The values of the thermodynamic functions of reactions (R1)-(R4) in the standard state (T = 298 K and $P = 10^5$ Pa) were calculated according to Eq 2-4 and are listed in the Table 3.

The Gibbs energies of reactions (R1) and (R2) are related to the standard Gibbs energies of compounds by Eq 5 and 6:

$$\Delta_{r(R1)}G^\circ = 2\Delta_f G^\circ_{AgGa_5Te_8} - 5\Delta_f G^\circ_{Ga_2Te_5}, \quad \text{(Eq 5)}$$

$$\Delta_{r(R2)}G^\circ = 4\Delta_f G^\circ_{AgGa_5Te_8} - 9\Delta_f G^\circ_{Ga_2Te_3} - \Delta_f G^\circ_{Ga_2Te_5}. \quad \text{(Eq 6)}$$

By solving the system of Eq 5 and 6 one obtains:

$$\Delta_f G^\circ_{Ga_2Te_5} = \frac{\Delta_{r(R2)}G^\circ - 2\Delta_{r(R1)}G^\circ}{9} + \Delta_f G^\circ_{Ga_2Te_3}. \quad \text{(Eq 7)}$$

Equations for determining the enthalpy of formation and entropy of the Ga_2Te_5 compound were similarly obtained:

$$\Delta_f H^\circ_{Ga_2Te_5} = \frac{\Delta_{r(R2)}H^\circ - 2\Delta_{r(R1)}H^\circ}{9} + \Delta_f H^\circ_{Ga_2Te_3}, \quad \text{(Eq 8)}$$

$$S^\circ_{Ga_2Te_5} = \frac{\Delta_{r(R2)}S^\circ - 2\Delta_{r(R1)}S^\circ}{9} + 2S^\circ_{Te} + S^\circ_{Ga_2Te_3}. \quad \text{(Eq 9)}$$

Reactions to determine the standard thermodynamic properties $\Delta_f G^\circ$, $\Delta_f H^\circ$, and S° of the $AgGa_5Te_8$, Ga_7Te_{10}, and Ga_3Te_4 compounds were written in a similar way using reactions (R2)-(R4) with the corresponding stoichiometric numbers.

For the first time, the standard thermodynamic values for compounds of the GaTe-$AgGa_5Te_8$-Te system were determined using Eq 7-9 and the thermodynamic data of pure substances (Ag, Ga, Te) and the binary compound Ga_2Te_3.[54] The results of the calculations are listed in Table 4.

The temperature dependences of the Gibbs energies of the formation of compounds of the GaTe-$AgGa_5Te_8$-Te system are described by Eq 10-13:

Table 3 The values of standard thermodynamic functions of reactions (R1)-(R4). Standard uncertainties for $\Delta_r G^\circ$, $\Delta_r H^\circ$, and $\Delta_r S^\circ$ are also listed

Reactions	$-\Delta_r G^\circ$, kJ mol^{-1}	$-\Delta_r H^\circ$	$\Delta_r S^\circ$, J (mol K)$^{-1}$
(R1)	49.14 ± 0.05	40.40 ± 0.15	29.33 ± 0.34
(R2)	108.42 ± 0.15	94.90 ± 0.49	45.38 ± 1.15
(R3)	23.70 ± 0.04	20.39 ± 0.19	11.09 ± 0.50
(R4)	23.29 ± 0.04	20.30 ± 0.15	10.03 ± 0.35

$$\frac{\Delta_f G_{Ga_2Te_5}}{(kJmol^{-1})} = -(276.5 \pm 4.6) + (18.1 \pm 0.3) \times \frac{10^{-3}T}{K}, \quad \text{(Eq 10)}$$

$$\frac{\Delta_f G_{AgGa_5Te_8}}{(kJmol^{-1})} = -(711.3 \pm 8.8) + (30.9 \pm 0.4) \times \frac{10^{-3}T}{K}, \quad \text{(Eq 11)}$$

$$\frac{\Delta_f G_{Ga_7Te_{10}}}{(kJmol^{-1})} = -(958.4 \pm 11.7) + (58.6 \pm 0.7) \times \frac{10^{-3}T}{K}, \quad \text{(Eq 12)}$$

$$\frac{\Delta_f G_{Ga_3Te_4}}{(kJmol^{-1})} = -(408.6 \pm 7.9) + (25.4 \pm 0.4) \times \frac{10^{-3}T}{K}. \quad \text{(Eq 13)}$$

The obtained $\Delta_f G^\circ_{Ga_2Te_5}$, $\Delta_f G^\circ_{AgGa_5Te_8}$, $\Delta_f G^\circ_{Ga_7Te_{10}}$, and $\Delta_f G^\circ_{Ga_3Te_4}$ values do not exclude the hypothetical reactions of the synthesis of compounds under standard conditions:

$$Ga_2Te_3 + 2Te = Ga_2Te_5, \quad \text{(Eq R5)}$$

$$Ag_2Te + 5Ga_2Te_3 = 2AgGa_5Te_8, \quad \text{(Eq R6)}$$

$$GaTe + 3Ga_2Te_3 = Ga_7Te_{10}, \quad \text{(Eq R7)}$$

$$GaTe + Ga_2Te_3 = Ga_3Te_4. \quad \text{(Eq R8)}$$

Table 4 The values of standard (T = 298 K and P = 10^5 Pa) thermodynamic properties of compounds of the GaTe-$AgGa_5Te_8$-Te system

Phases	$-\Delta_f G^\circ$, kJ mol^{-1}	$-\Delta_f H^\circ$	S°, J $(mol\ K)^{-1}$	[Ref]
Ag	0	0	42.677	[54]
Ga	0	0	40.828	[54]
Te	0	0	49.497	[54]
Ga_2Te_3	269.892	274.889	213.384	[54]
Ga_2Te_5	271.1 ± 3.4	276.5 ± 4.6	310.9 ± 4.5	This work
$AgGa_5Te_8$	702.1 ± 7.8	711.3 ± 8.8	611.9 ± 7.6	This work
Ga_7Te_{10}	940.9 ± 10.9	958.4 ± 11.7	722.2 ± 8.8	This work
Ga_3Te_4	401.0 ± 5.9	408.6 ± 7.9	295.1 ± 4.7	This work

Standard uncertainties for $\Delta_f G^\circ$, $\Delta_f H^\circ$, and S° are also listed.

The calculated values of Gibbs energies of the reaction (R5)-(R8) $\Delta_{r(R5)}G^\circ = -1.2$ kJmol^{-1}, $\Delta_{r(R6)}G^\circ = -19.6$ kJmol^{-1}, $\Delta_{r(R7)}G^\circ = -9.3$ kJmol^{-1}, and $\Delta_{r(R8)}G^\circ = -9.2$ kJmol^{-1} are negative. Thus, the standard thermodynamic values of compounds presented in Table 4 do not contradict the thermodynamics laws.

3.2 Phase Equilibria and Thermodynamic Properties of Quaternary Compounds of the Ag-Ga-Te-AgBr System Below 600 K

The division of composition space of the Ag-Ga-Te-AgBr system in the Ag_2Te-GaTe-Te-AgBr-Ag_2Te part is shown in Fig. 5(a)-(e). The triangulation is performed according to:

1) the results of the E versus T dependencies of the ECs with PE of different phase regions;
2) the established phase composition of the GaTe-$AgGa_5Te_8$-Te phase region (see Section 3.1); and
3) the existence of quaternary compounds in the AgTe-Ga_2Te_3-AgBr system.

The locations of individual tetrahedra Ga_2Te_3-Ga_2Te_5-AgBr-$Ag_3Ga_{10}Te_{16}Br$ (phase region (V)), Ga_2Te_3-AgBr-$Ag_3Ga_{10}Te_{16}Br$-Ga_7Te_{10} (VI), Ga_7Te_{10}-AgBr-$Ag_3Ga_{10}Te_{16}Br$-Ga_3Te_4 (VII), $Ag_3Ga_{10}Te_{16}Br$-Ga_2Te_5-AgBr-$Ag_3Ga_2Te_4Br$ (VIII), $Ag_3Ga_{10}Te_{16}Br$-AgBr-$Ag_3Ga_2Te_4Br$-GaTe (IX), $Ag_3Ga_2Te_4Br$-AgBr-$Ag_{27}Ga_2Te_{12}Br_9$-GaTe (X), and Ga_2Te_5-AgBr-$Ag_3Ga_2Te_4Br$-$Ag_{27}Ga_2Te_{12}Br_9$ (XI) of the Ag_2Te-GaTe-Te-AgBr-Ag_2Te part are shown in Fig. 5(b)-(e). All of these tetrahedra contain quaternary compounds. The spatial position of four-phase regions (V)-(XI) relative to the silver point was used to establish the overall potential-determining reactions of synthesis of the quaternary compounds. The common planes between two tetrahedra are illustrated as shaded areas in Fig. 5(b), (d) and (e).

The reactions for these individual phase regions can be described as follows

According to Fig. 5(b), reactions (R9) and (R10) for the phase regions (V) and (VI), respectively, can be expressed as:

$$4Ag + 9Ga_2Te_3 + Ga_2Te_5 + AgBr = 2Ag_3Ga_{10}Te_{16}Br, \quad \text{(Eq R9)}$$

$$2Ag + 12Ga_2Te_3 + AgBr = Ag_3Ga_{10}Te_{16}Br + 2Ga_7Te_{10}, \quad \text{(Eq R10)}$$

the common plane for these phase regions is $Ag_3Ga_{10}Te_{16}Br$-Ga_2Te_3-AgBr;

for phase region (VII), Fig. 5(c):

$$2Ag + 4Ga_7Te_{10} + AgBr = Ag_3Ga_{10}Te_{16}Br + 6Ga_3Te_4; \quad \text{(Eq R11)}$$

for the phase regions (VIII) and (IX), Fig. 5(d):

$$16Ag + 4Ga_2Te_5 + 8AgBr + Ag_3Ga_{10}Te_{16}Br = 9Ag_3Ga_2Te_4Br, \quad \text{(Eq R12)}$$

$$4Ag + Ag_3Ga_{10}Te_{16}Br + 2AgBr = 3Ag_3Ga_2Te_4Br + 4GaTe, \quad \text{(Eq R13)}$$

the common plane is $Ag_3Ga_{10}Te_{16}Br$-$3Ag_3Ga_2Te_4Br$-AgBr;

for the phase regions (X) and (XI), Fig. 5(e):

$$8Ag + 5Ag_3Ga_2Te_4Br + 4AgBr = Ag_{27}Ga_2Te_{12}Br_9 + 8GaTe, \quad \text{(Eq R14)}$$

$$32Ag + 8Ga_2Te_5 + 16AgBr = Ag_{27}Ga_2Te_{12}Br_9 + 7Ag_3Ga_2Te_4Br, \quad \text{(Eq R15)}$$

the common plane is $Ag_3Ga_2Te_4Br$-AgBr-$Ag_{27}Ga_2Te_{12}Br_9$.

According to these reactions, ratios of binary compounds in the PE of ECs were calculated. Quaternary compounds are presented in heterophase mixtures of PE by the following binary phases: $Ag_3Ga_{10}Te_{16}Br \rightarrow Ag_2Te$,

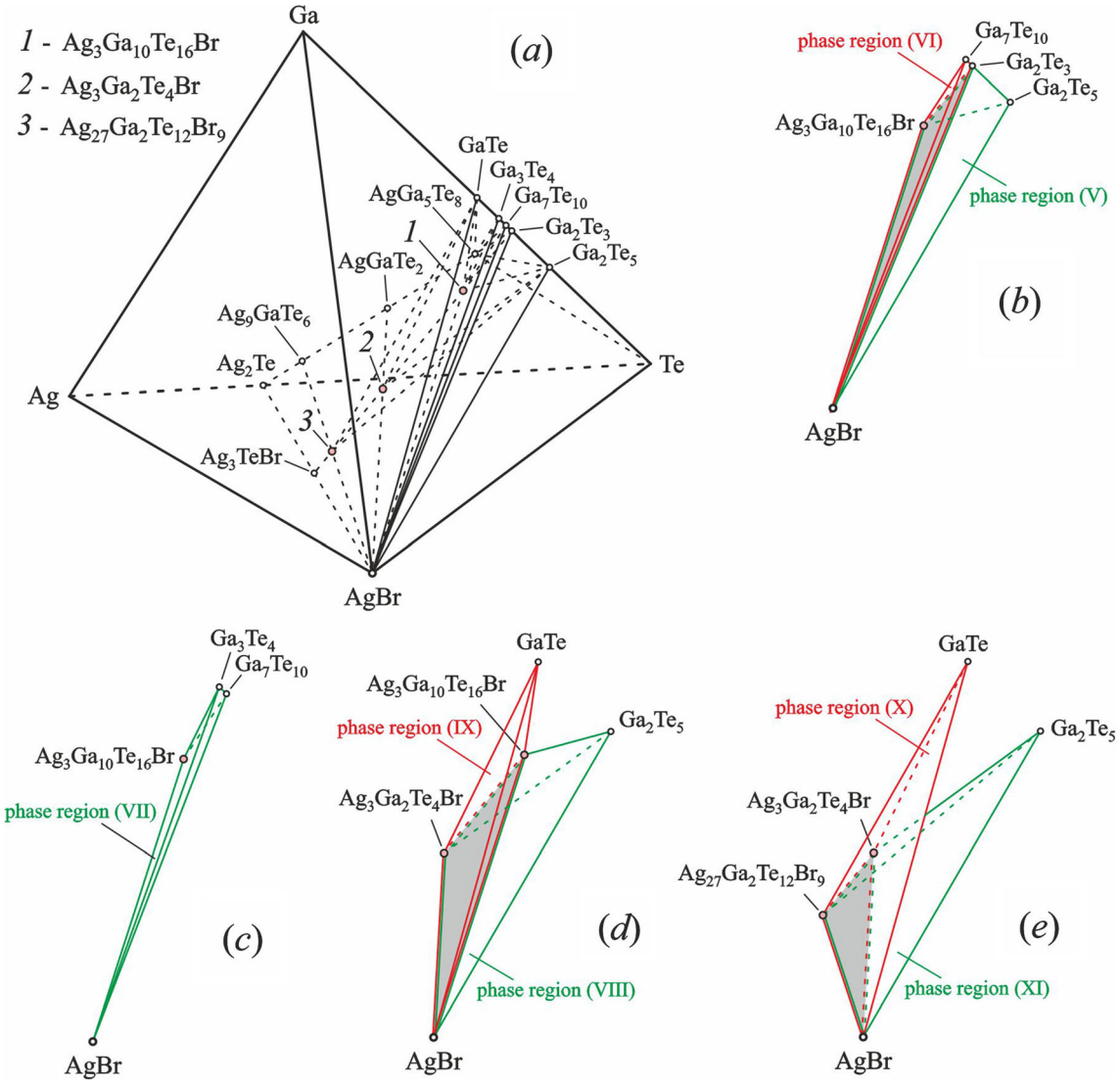

Fig. 5. Divisions of composition space of the Ag-Ga-Te-AgBr system in the Ag_2Te-GaTe-Te-AgBr-Ag_2Te part on separate phase regions below 600 K

$5Ga_2Te_3$, and AgBr; $Ag_3Ga_2Te_4Br \rightarrow Ag_2Te$, Ga_2Te_3, and AgBr; $Ag_{27}Ga_2Te_{12}Br_9 \rightarrow 9Ag_2Te$, Ga_2Te_3, and 9AgBr.

Experimental quantities of temperature and EMF of the ECs with PE of the phase regions (V)-(XI) are listed in Table 5.

The experimental values of T and E listed in Table 5 were used to calculate the coefficients and statistical dispersions of Eq 1 for the phase regions (V)-(XI). The results of the calculations are listed in Table 6.

The values of the thermodynamic functions of reactions (R9)-(R15) in the standard state (T = 298 K and $P = 10^5$ Pa) were calculated according to Eq 2-4 and are listed in Table 7.

The standard thermodynamic properties of the quaternary compounds of the Ag-Ga-Te-AgBr system were calculated in a similar way to the ternary and binary compounds of the Ag-Ga-Te system (see Section 3.1). The results of the calculations are listed in Table 8.

The determined Gibbs energy values of the quaternary compounds $Ag_3Ga_{10}Te_{16}Br$ in the phase regions (V), (VI), (VII) and $Ag_3Ga_2Te_4Br$ in regions (VIII), (IX) are the same within the experimental errors. The standard Gibbs energy of formation of the $Ag_{27}Ga_2Te_{12}Br_9$ compound calculated using (R14) $\Delta_f G^\circ_{Ag_{27}Ga_2Te_{12}Br_9,(R14)} = -1629.9 kJmol^{-1}$ differs significantly from the value obtained from (R15) $\Delta_f G^\circ_{Ag_{27}Ga_2Te_{12}Br_9,(R15)} = -1492.5 kJmol^{-1}$. To analyze the obtained values from a thermodynamic point of view, the Gibbs energy of a hypothetical reaction

Table 5 Measured values of temperature (T) and EMF (E) of the ECs with PE of different phase regions at pressure $P = 10^5$ Pa

T/K	Phase region						
	(V) E/mV	(VI) E/mV	(VII) E/mV	(VIII) E/mV	(IX) E/mV	(X) E/mV	(XI) E/mV
350.3	255.4	231.7	227.3	233.6	226.5	211.0	220.4
355.3	256.1	232.4	228.1	234.0	227.0	211.9	220.9
360.3	256.8	233.2	229.0	234.7	227.5	212.8	221.7
365.4	257.5	233.9	229.7	235.2	228.1	213.6	222.3
370.4	258.4	234.7	230.6	235.7	228.8	214.5	223.1
375.4	259.1	235.5	231.6	236.2	229.3	215.4	223.8
380.4	259.9	236.3	232.5	236.7	229.9	216.3	224.5
385.4	260.6	237.0	233.3	237.2	230.5	217.2	225.2
390.4	261.3	237.7	234.2	237.7	231.1	218.0	226.0
395.4	262.0	238.4	235.0	238.2	231.6	218.9	226.8
400.4	262.7	239.2	235.7	238.7	232.3	219.7	227.5
405.4	263.4	239.9	236.4	239.2	232.9	220.6	228.3

Standard uncertainties u are $u(T) = 0.5$ K, $u(P) = 10^4$ Pa, and $u(E) = 0.3$ mV.

Table 6 The coefficients and statistical dispersions of E versus T dependencies of the ECs

Phase regions	$E = a + bT \pm k_{St}\sqrt{\left(\frac{u_E^2}{n} + u_b^2(T-\overline{T})^2\right)}$
(V)	$E = 203.99 + 146.72 \times 10^{-3}T \pm 2.179\sqrt{\left(\frac{3.98\times10^{-3}}{12} + 1.11 \times 10^{-6}(T-377.88)^2\right)}$
(VI)	$E = 179.25 + 149.72 \times 10^{-3}T \pm 2.179\sqrt{\left(\frac{2.37\times10^{-3}}{12} + 6.61 \times 10^{-7}(T-377.88)^2\right)}$
(VII)	$E = 168.12 + 168.91 \times 10^{-3}T \pm 2.179\sqrt{\left(\frac{1.25\times10^{-2}}{12} + 3.48 \times 10^{-6}(T-377.88)^2\right)}$
(VIII)	$E = 197.94 + 101.84 \times 10^{-3}T \pm 2.179\sqrt{\left(\frac{2.61\times10^{-3}}{12} + 7.29 \times 10^{-7}(T-377.88)^2\right)}$
(IX)	$E = 185.45 + 116.91 \times 10^{-3}T \pm 2.179\sqrt{\left(\frac{3.41\times10^{-3}}{12} + 9.49 \times 10^{-7}(T-377.88)^2\right)}$
(X)	$E = 150.02 + 174.15 \times 10^{-3}T \pm 2.179\sqrt{\left(\frac{1.38\times10^{-3}}{12} + 3.85 \times 10^{-7}(T-377.88)^2\right)}$
(XI)	$E = 169.48 + 144.83 \times 10^{-3}T \pm 2.179\sqrt{\left(\frac{8.11\times10^{-3}}{12} + 2.26 \times 10^{-6}(T-377.88)^2\right)}$

$$9Ag_2Te + Ga_2Te_5 + 9AgBr = Ag_{27}Ga_2Te_{12}Br_9, \quad \text{(Eq R16)}$$

of formation of the quaternary compound from the binary compounds was calculated by Eq 14:

$$\Delta_{r(R16)}G^\circ = \Delta_f G^\circ_{Ag_{27}Ga_2Te_{12}Br_2} - 9\Delta_f G^\circ_{Ag_2Te} - \Delta_f G^\circ_{Ga_2Te_5} - 9\Delta_f G^\circ_{AgBr}. \quad \text{(Eq 14)}$$

Considering data from Ref.[54] $\Delta_f G^\circ_{Ag_2Te} = -41.558\text{kJmol}^{-1}$, $\Delta_f G^\circ_{Ga_2Te_5} = -271.019\text{kJmol}^{-1}$, $\Delta_f G^\circ_{AgBr} = -97.095\text{kJmol}^{-1}$ it was found that

Table 7 The values of standard thermodynamic properties of the reactions (R9)-(R15)

Reactions	$-\Delta_r G^\circ$, kJ mol^{-1}	$-\Delta_r H^\circ$	$\Delta_r S^\circ$, J (mol K)$^{-1}$
(R9)	95.60 ± 0.07	78.73 ± 0.34	56.63 ± 0.89
(R10)	43.20 ± 0.03	34.59 ± 0.13	28.89 ± 0.34
(R11)	42.16 ± 0.06	32.44 ± 0.30	32.59 ± 0.78
(R12)	352.42 ± 0.23	305.57 ± 1.09	157.22 ± 2.87
(R13)	85.02 ± 0.07	71.57 ± 0.31	45.12 ± 0.82
(R14)	155.86 ± 0.09	115.80 ± 0.40	134.42 ± 1.04
(R15)	656.53 ± 0.83	523.28 ± 3.84	447.17 ± 10.12

Uncertainties for $\Delta_r G^\circ$, $\Delta_r H^\circ$, and $\Delta_r S^\circ$ are standard uncertainties.

Table 8 The values of standard (T = 298 K and P = 10^5 Pa) thermodynamic properties of selected compounds of the Ag-Ga-Te-AgBr system

Phases	Phase region	Reaction	$-\Delta_f G^\circ$ kJ mol^{-1}	$-\Delta_f H^\circ$	S° J $(mol\ K)^{-1}$	[Ref.]
Br_2	…	…	0	0	152.210	[54]
AgBr	…	…	97.095	100.575	107.110	[54]
$Ag_3Ga_{10}Te_{16}Br$	(V)	(R9)	1494.9 ± 28.9	1515.2 ± 41.2	1336.5 ± 37.8	This work
$Ag_3Ga_{10}Te_{16}Br$	(VI)	(R10)	1497.1 ± 29.3	1517.1 ± 41.5	1337.5 ± 38.0	This work
$Ag_3Ga_{10}Te_{16}Br$	(VII)	(R11)	1496.9 ± 29.1	1515.1 ± 41.2	1343.4 ± 38.2	This work
$Ag_3Ga_2Te_4Br$	(VIII)	(R12)	412.2 ± 8.9	414.6 ± 10.1	476.0 ± 11.7	This work
$Ag_3Ga_2Te_4Br$	(IX)	(R13)	429.4 ± 9.2	431.4 ± 10.5	477.3 ± 11.8	This work
$Ag_{27}Ga_2Te_{12}Br_9$	(X)	(R14)	1629.9 ± 31.9	1603.5 ± 34.2	2601.4 ± 54.7	This work

Uncertainties for $\Delta_f G^\circ$, $\Delta_f H^\circ$, and S° are standard uncertainties.

$\Delta_{r(R16)}G^\circ < 0$ using the value of $\Delta_f G^\circ_{Ag_{27}Ga_2Te_{12}Br_9,(R14)}$ and $\Delta_{r(R16)}G^\circ > 0$ using the value of $\Delta_f G^\circ_{Ag_{27}Ga_2Te_{12}Br_9,(R15)}$. Consequently, the $\Delta_f G^\circ_{Ag_{27}Ga_2Te_{12}Br_9,(R15)}$ value contradicts the thermodynamics laws. This means that in PE of ECs the mixture of compounds formed with the participation of the catalyst Ag^+ does not correspond to that expressed in (R15). it is likely that the Ga_2Te_5 compound in the set of phases in (R15) is not formed for thermodynamic reasons. The experimentally established participation of the Ga_2Te_5 in the divisions of the GaTe-$AgGa_5Te_8$-Te region below 600 K indicates the possibility of its existence as a thermodynamically stable compound in the aggregate of three phases of PE—reactions (R1) and (R2), as well as four phases of PE—reaction (R9). Similar properties were established for the metastable phases Ag_5Te_2Br of the Ag-Te-Br system and Ag_2NiSnS_4 of the Ag-Ni-Sn-S system.[39,40]

4 Conclusions

The EMF method was applied to divide the $T - x$ space of the Ag-Ga-Te-AgBr system in the Ag_2Te-GaTe-Te-AgBr-Ag_2Te part below 600 K into three- and four-phase regions with the participation of stable Ga_3Te_4, Ga_7Te_{10}, $AgGa_5Te_8$, $Ag_3Ga_{10}Te_{16}Br$, $Ag_3Ga_2Te_4Br$, $Ag_{27}Ga_2Te_{12}Br_9$ and metastable Ga_2Te_5 compounds. The $AgGa_2Te_3Br$ compound did not form below 600 K. The synthesis of the equilibrium set of phases using the calculated amounts of binary compounds Ag_2Te, GaTe, Ga_2Te_3, AgBr, and pure Te was carried out in the positive electrodes of electrochemical cells with the participation of the Ag^+ catalysts. The standard thermodynamic functions (Gibbs energies, enthalpies, and entropies) for the compounds Ga_2Te_5, Ga_7Te_{10}, Ga_3Te_4, $AgGa_5Te_8$, $Ag_3Ga_{10}Te_{16}Br$, $Ag_3Ga_2Te_4Br$, and $Ag_{27}Ga_2Te_{12}Br_9$ were determined by the EMF method, for the first time. The obtained values of the Gibbs energies of formation of the compounds are in accordance with the laws of thermodynamics. Based on x-ray diffraction phase analysis and EMF measurements of the electrochemical cells, it was concluded that compounds Ga_7Te_{10} and $AgGa_5Te_8$ exist in two temperature ranges. The established existence of two-phase equilibria between the compounds along the cross-sections $AgGa_5Te_8$-$Ag_3Ga_{10}Te_{16}Br$, $AgGaTe_2$-$Ag_3Ga_2Te_4Br$, and Ag_9GaTe_6-$Ag_{27}Ga_2Te_{12}Br_9$ allows the formation of solid solutions based on them. The formation of solid solutions is an effective strategy for increasing the thermoelectric figure of merit ZT parameters of different materials.

Acknowledgments The present work was financed partially by the grant of the Ministry of Education and Science of Ukraine No. 0123U101857 "Physico-chemistry of functional nanomaterials for electrochemical systems", international projects: #HX-010123 from ''Materials Phases Data System, Viznau, Switzerland'' and the Simons Foundation (Award Number: 1037973). This work was partly funded by the K.H. Renlund Foundation under the project "Innovative e-waste recycling processes for greener and more efficient recoveries of critical metals and energy" at Åbo Akademi University.

Conflict of interest The authors declare that they have no conflict of interest.

References

1. T.P. Bailey and C. Uher, Potential for Superionic Conductors in Thermoelectric Applications, *Curr. Opin. Green Sustain. Chem.*, 2017, **4**, p 58-63. https://doi.org/10.1016/j.cogsc.2017.02.007
2. W. Liu, J. Hu, S. Zhang, M. Deng, C.-G. Han, and Y. Liu, New Trends, Strategies and Opportunities in Thermoelectric Materials: A Perspective, *Mater. Today Phys.*, 2017, **1**, p 50-60. https://doi.org/10.1016/j.mtphys.2017.06.001
3. Y. Shi, C. Sturm, and H. Kleinke, Chalcogenides as Thermoelectric Materials, *J. Solid State Chem.*, 2019, **270**, p 273-279. https://doi.org/10.1016/j.jssc.2018.10.049
4. R.M. Sardarly, G.M. Ashirov, L.F. Mashadiyeva, N.A. Aliyeva, F.T. Salmanov, R.S. Agayeva, R.A. Mamedov, and M.B.

Babanly, Ionic Conductivity of the Ag_8GeSe_6 Compound, *Mod. Phys. Lett. B*, 2022, **36**(32-33), p 2250171. https://doi.org/10.1142/S0217984922501718
5. S.Y. Tee, D. Ponsford, C.L. Lay, X. Wang, X. Wang, D.C. Neo, T. Wu, W. Thitsartarn, J.C. Yeo, G. Guan, T.-C. Lee, and M.-Y. Han, Thermoelectric Silver-Based Chalcogenides, *Adv. Sci.*, 2022, **9**(36), p 2204624. https://doi.org/10.1002/advs.202204624
6. W. Zhou, J. Wu, W. Liu, and S.-P. Guo, Ag-Based Chalcogenides and Derivatives as Promising Infrared Nonlinear Optical Materials, *Coord. Chem. Rev.*, 2023, **477**(1-15), p 214950. https://doi.org/10.1016/j.ccr.2022.214950
7. M.V. Moroz and M.V. Prokhorenko, Thermodynamic Properties of the Intermediate Phases of the Ag-Sb-Se System, *Russ. J. Phys. Chem. A*, 2014, **88**(5), p 742-746. https://doi.org/10.1134/S0036024414050203
8. L.F. Mashadieva, J.O. Kevser, I.I. Aliev, Y.A. Yusibov, D.B. Tagiyev, Z.S. Aliev, and M.B. Babanly, Phase Equilibria in the Ag_2Te-SnTe-Sb_2Te_3 System and Thermodynamic Properties of the $(2SnTe)_{1-x}(AgSbTe_2)_x$ Solid Solution, *J. Phase Equilibria Diffus.*, 2017, **38**, p 603-614. https://doi.org/10.1007/s11669-017-0583-2
9. T.V. Vu, A.A. Lavrentyev, B.V. Gabrelian, V.A. Ocheretova, O.V. Parasyuk, and O.Y. Khyzhun, Particular Features of the Electronic Structure and optical Properties of Ag_2PbGeS_4 as Evidenced from First-Principles DFT Calculations and XPS Studies, *Mater. Chem. Phys.*, 2018, **208**, p 268-280. https://doi.org/10.1016/j.matchemphys.2018.01.042
10. A.O. Selezen, I.D. Olekseyuk, G.L. Myronchuk, O.V. Smitiukh, and L.V. Piskach, Synthesis and Structure of the New Semiconductor Compounds $Tl_2B^{II}D^{IV}X_4$ (B^{II}-Cd, Hg; D^{IV}-Si, Ge; X-Se, Te) and Isothermal Sections of the Tl_2Se-CdSe-Ge(Sn)Se_2 Systems at 570 K, *J. Solid State Chem.*, 2020, **289**, 121422. https://doi.org/10.1016/j.jssc.2020.121422
11. I.A. Ivashchenko, O.S. Klymovych, I.D. Olekseyuk, L.D. Gulay, V.V. Halyan, and O.M. Strok, Quasi-Ternary System Ag_2Se-$GeSe_2$-As_2Se_3, *J. Phase Equilibria Diffus.*, 2022, **43**(4), p 483-494. https://doi.org/10.1007/s11669-022-00987-0
12. I. Semkiv, H. Ilchuk, M. Pawlowski, and V. Kusnezh, Ag_8SnSe_6 Argyrodite Synthesis and Optical Properties, *Opto-Electron. Rev.*, 2017, **25**(1), p 37-40. https://doi.org/10.1016/j.opelre.2017.04.002
13. O.H. Ando Junior, A.L.O. Maran, and N.C. Henao, A review of the development and applications of thermoelectric microgenerators for energy harvesting, *Renew. Sustain. Energy Rev.*, 2018, **91**, p 376-393. https://doi.org/10.1016/j.rser.2018.03.052
14. S. Hooshmand Zaferani, M. Jafarian, D. Vashaee, and R. Ghomashchi, Thermal Management Systems and Waste Heat Recycling by Thermoelectric Generators—An Overview, *Energies*, 2021, **14**(18), p 5646. https://doi.org/10.3390/en14185646
15. A.O. Ochieng, T.F. Megahed, S. Ookawara, and H. Hassan, Comprehensive Review in Waste Heat Recovery in Different Thermal Energy-Consuming Processes Using Thermoelectric Generators for Electrical Power Generation, *Process. Saf. Environ. Prot.*, 2022, **162**, p 134-154. https://doi.org/10.1016/j.psep.2022.03.070
16. R. Freer and A.V. Powell, Realising the Potential of Thermoelectric Technology: A Roadmap, *J. Mater. Chem. C*, 2020, **8**(2), p 441-463. https://doi.org/10.1039/C9TC05710B
17. G.S. Hasanova, A.I. Aghazade, S.Z. Imamaliyeva, Y.A. Yusibov, and M.B. Babanly, Refinement of the Phase Diagram of the Bi-Te System and the Thermodynamic Properties of Lower Bismuth Tellurides, *JOM*, 2021, **73**(5), p 1511-1521. https://doi.org/10.1007/s11837-021-04621-1
18. X. Zeng, C. Yan, L. Ren, T. Zhang, F. Zhou, X. Liang, N. Wang, R. Sun, J.-B. Xu, and C.-P. Wong, Silver Telluride Nanowire Assembly for High-Performance Flexible Thermoelectric Film and its Application in Self-Powered Temperature Sensor, *Adv. Electron. Mater*, 2019, **5**(2), p 1800612. https://doi.org/10.1002/aelm.201800612
19. T. Takabatake, K. Suekuni, T. Nakayama, and E. Kaneshita, Phonon-Glass Electron-Crystal Thermoelectric Clathrates: Experiments and Theory, *Rev. Mod. Phys.*, 2014, **86**(2), p 669-716. https://doi.org/10.1103/RevModPhys.86.669
20. M. Beekman, D.T. Morelli, and G.S. Nolas, Better Thermoelectrics Through Glass-Like Crystals, *Nat. Mater.*, 2015, **14**(12), p 1182-1185. https://doi.org/10.1038/nmat4461
21. M.J. Filep, A.I. Pogodin, M.M. Luchynets, and I.P. Studenyak, Thermoelectric Parameters of Single Crystals with Argyrodite Structure in Cu_7PS_6-Cu_6PS_5Br and Cu_7PS_6-Cu_6PS_5I Systems, *Uzhhorod Univ. Sci, Herald. Ser. Phys.*, 2020, **40**, p 44-51. **(in Ukrainian)**
22. S. Drzewowska and B. Onderka, Different Approach to Thermodynamic Description of Bi-Te Binary System, *J. Phase Equilibria Diffus.*, 2023, **44**(3), p 429-444. https://doi.org/10.1007/s11669-023-01049-9
23. R. Blachnik and H.A. Dreisbach, The Phase Diagrams of Ag_2X-AgY (X = S, Se, Te; Y = Cl, Br, I): Mixtures and the Structure of Ag_5Te_2Cl, *J. Solid State Chem.*, 1985, **60**(1), p 115–122. https://doi.org/10.1016/0022-4596(85)90171-9
24. V. Kramer, H. Hirth, M. Hofherr, and H.-P. Trah, Phase Studies in the Systems Ag_2Te-Ga_2Te_3, ZnSe-In_2Se_3 and ZnS-Ga_2S_3, *Thermochim. Acta*, 1987, **112**(1), p 88–94. https://doi.org/10.1016/0040-6031(87)88085-1
25. I.A. Ivashchenko, V.S. Kozak, L.D. Gulay, and V.V. Galyan, Phase Equilibria in the Quasi-Ternary System Cu_2Se-In_2Se_3-CuI and the Crystal Structure of the $A^IB^{III}{}_2X^{VI}{}_3Y^{VII}$ Compounds, Where A^I-Cu, Ag; B^{III}-Ga; X^{VI}-Cl, Br, I; Y^{VII}-S, Se, Te, *J. Phase Equilibria Diffus.*, 2023, **44**(6), p 714–728. https://doi.org/10.1007/s11669-023-01073-9
26. M. Guittard, J. Rivet, F. Alapini, A. Chilouet, and A.-M. Loireau-Lozac'h, Description du Système Ternaire Ag-Ga-Te, *J. Common Met.*, 1991, **170**(2), p 373–392. https://doi.org/10.1016/0022-5088(91)90339-6
27. H.J. Deiseroth and H.-D. Müller, Crystal Structures of heptagallium Decatelluride, Ga_7Te_{10} and Heptaindium Decatelluride, In_7Te_{10}, *Z. Für Krist. Cryst. Mater.*, 1995, **210**(1), p 57–58. https://doi.org/10.1524/zkri.1995.210.1.57
28. C. Julien, I. Ivanov, A. Khelfa, F. Alapini, and M. Guittard, Characterization of the Ternary Compounds $AgGaTe_2$ and $AgGa_5Te_8$, *J. Mater. Sci.*, 1996, **31**(12), p 3315–3319. https://doi.org/10.1007/BF00354684
29. R. Blachnik, and E. Klose, Experimental Investigation and Thermodynamic Calculation of Excess Enthalpies in the Ga-In-Te System, *J. Alloys Compd.*, 2000, **305**(1–2), p 144–152. https://doi.org/10.1016/S0925-8388(00)00695-2
30. A. Charoenphakdee, K. Kurosaki, H. Muta, M. Uno, and S. Yamanaka, Thermal Conductivity of the Ternary Compounds: $AgMTe_2$ and AgM_5Te_8 (M=Ga or In), *Mater. Trans.*, 2009, **50**(7), p 1603–1606. https://doi.org/10.2320/matertrans.E-M2009810
31. S. Lin, W. Li, Z. Bu, B. Shan, and Y. Pei, Thermoelectric *p*-Type Ag_9GaTe_6 with an Intrinsically Low Lattice Thermal Conductivity, *ACS Appl. Energy Mater.*, 2020, **3**(2), p 1892–1898. https://doi.org/10.1021/acsaem.9b02330
32. M.V. Moroz, P. Demchenko, M.V. Prokhorenko, and O.V. Reshetnyak, Thermodynamic Properties of Saturated Solid Solutions of the Phases Ag_2PbGeS_4, $Ag_{0.5}Pb_{1.75}GeS_4$ and $Ag_{6.72}Pb_{0.16}Ge_{0.84}S_{5.20}$ of the Ag-Pb-Ge-S System Determined by EMF Method, *J. Phase Equilibria Diffus.*, 2017, **38**(4), p 426–433. https://doi.org/10.1007/s11669-017-0563-6
33. M.V. Moroz, M.V. Prokhorenko, O.V. Reshetnyak, and PYu. Demchenko, Electrochemical Determination of Thermodynamic Properties of Saturated Solid Solutions of Hg_2GeSe_3, Hg_2GeSe_4,

$Ag_2Hg_3GeSe_6$, and $Ag_{1.4}Hg_{1.3}GeSe_6$ Compounds in the Ag-Hg-Ge-Se System, *J. Solid State Electrochem.*, 2017, **21**(3), p 833–837. https://doi.org/10.1007/s10008-016-3424-z
34. Diffractometer Stoe WinXPOW, Version 3.03, Stoe & Cie GmbH, Darmstadt, 2010
35. W. Kraus and G. Nolze, POWDER CELL—A Program for the Representation and Manipulation of Crystal Structures and Calculation of the Resulting x-ray Powder Patterns, *J. Appl. Crystallogr.*, 1996, **29**, p 301–303. https://doi.org/10.1107/S0021889895014920
36. J. Rodriguez-Carvajal, Recent Developments of the Program FULLPROF, *IUCr Comm. Powder Diffr. Newsl.*, 2001, **26**, p 12–19.
37. R.T. Downs and M. Hall-Wallace, The American Mineralogist Crystal Structure Database, *Am. Miner.*, 2003, **88**, p 247–250.
38. P. Villars and K. Cenzual (Eds.), *Pearson's Crystal Data: Crystal Structure Database for Inorganic Compounds, Release 2021/22*, ASM International, Materials Park (Ohio, USA), 2012
39. M. Moroz, F. Tesfaye, P. Demchenko, M. Prokhorenko, S. Prokhorenko, and O. Reshetnyak, Non-Activation Synthesis and Thermodynamic Properties of Ternary Compounds of the Ag-Te-Br System, *Thermochim. Acta*, 2021, **698**, p 178862. https://doi.org/10.1016/j.tca.2021.178862
40. M. Moroz, F. Tesfaye, P. Demchenko, V. Kordan, M. Prokhorenko, O. Mysina, O. Reshetnyak, and R. Gladyshevskii, Synthesis, Thermodynamic Properties, and Structural Characteristics of Multicomponent Compounds in the Ag-Ni-Sn-S System, *JOM*, 2023, **75**(6), p 2016–2025. https://doi.org/10.1007/s11837-023-05784-9
41. M.V. Moroz, PYu. Demchenko, O.G. Mykolaychuk, L.G. Akselrud, and R.E. Gladyshevskii, Synthesis and Electrical Conductivity of Crystalline and Glassy Alloys in the Ag_3GeS_3Br-GeS_2 System, *Inorg. Mater.*, 2013, **49**(9), p 867–871. https://doi.org/10.1134/S0020168513090100
42. M. Moroz, F. Tesfaye, P. Demchenko, M. Prokhorenko, D. Lindberg, O. Reshetnyak, and L. Hupa, Phase Equilibria and Thermodynamics of Selected Compounds in the Ag-Fe-Sn-S System, *J. Electron. Mater.*, 2018, **47**(9), p 5433–5442. https://doi.org/10.1007/s11664-018-6430-3
43. M.V. Moroz, M.V. Prokhorenko, and B.P. Rudyk, Thermodynamic Properties of Phases of the Ag-Ge-Te System, *Russ. J. Electrochem.*, 2014, **50**(12), p 1177–1181. https://doi.org/10.1134/S1023193514120039
44. M.V. Prokhorenko, M.V. Moroz, and P.Y. Demchenko, Measuring the Thermodynamic Properties of Saturated Solid Solutions in the Ag_2Te-Bi-Bi_2Te_3 System by the Electromotive Force Method, *Russ. J. Phys. Chem. A*, 2015, **89**(8), p 1330–1334. https://doi.org/10.1134/S0036024415080269
45. R. Blachnik and U. Stöter, The Phase Diagram AgI-ZnI_2, *Thermochim. Acta*, 1989, **145**, p 93–99. https://doi.org/10.1016/0040-6031(89)85129-9
46. M. Moroz, F. Tesfaye, P. Demchenko, M. Prokhorenko, Y. Kogut, O. Pereviznyk, S. Prokhorenko, and O. Reshetnyak, Solid-State Electrochemical Synthesis and Thermodynamic Properties of Selected Compounds in the Ag-FePb-Se System, *Solid State Sci.*, 2020, **107**, p 106344. https://doi.org/10.1016/j.solidstatesciences.2020.106344
47. M. Moroz, F. Tesfaye, P. Demchenko, M. Prokhorenko, N. Yarema, D. Lindberg, O. Reshetnyak, and L. Hupa, The Equilibrium Phase Formation and Thermodynamic Properties of Functional Tellurides in the Ag-Fe-Ge-Te System, *Energies*, 2021, **14**(5), p 1314. https://doi.org/10.3390/en14051314
48. M. Babanly, Y. Yusibov, and N. Babanly, The EMF Method with Solid-State Electrolyte in the Thermodynamic Investigation of Ternary Copper and Silver Chalcogenides. In *Electromotive Force and Measurement in Several Systems* (S. Kara, Ed.), InTech, 2011, p 57–78. https://doi.org/10.5772/28934
49. F.M. Mammadov, I.R. Amiraslanov, S.Z. Imamaliyeva, and M.B. Babanly, Phase Relations in the FeSe–$FeGa_2Se_4$–$FeIn_2Se_4$ System: Refinement of the Crystal Structures of $FeIn_2Se_4$ and $FeGaInSe_4$, *J. Phase Equilibria Diffus.*, 2019, **40**(6), p 787–796. https://doi.org/10.1007/s11669-019-00768-2
50. G.S. Hasanova, A.I. Aghazade, D.M. Babanly, S.Z. Imamaliyeva, Y.A. Yusibov, and M.B. Babanly, Experimental Study of the Phase Relations and Thermodynamic Properties of Bi-Se System, *J. Therm. Anal. Calorim.*, 2021, **147**, p 6403–6414. https://doi.org/10.1007/s10973-021-10975-0
51. N.B. Babanly, E.N. Orujlu, S.Z. Imamaliyeva, Y.A. Yusibov, and M.B. Babanly, Thermodynamic Investigation of Silver-Thallium Tellurides by EMF Method with Solid Electrolyte Ag_4RbI_5, *J. Chem. Thermodyn.*, 2019, **128**, p 78–86. https://doi.org/10.1016/j.jct.2018.08.012
52. S.Z. Imamaliyeva, S.S. Musayeva, D.M. Babanly, Y.I. Jafarov, D.B. Taghiyev, and M.B. Babanly, Determination of the Thermodynamic Functions of Bismuth Chalcoiodides by EMF Method with Morpholinium Formate as Electrolyte, *Thermochim. Acta*, 2019, **679**, p 178319. https://doi.org/10.1016/j.tca.2019.178319
53. F.J. Gravetter and L.B. Wallnau, *Statistics for the Behavioral Sciences*, 10th edn. Cengage Learning, Australia; United States, 2017.
54. I. Barin, *Thermochemical Data of Pure Substances*. Wiley, 1995. https://doi.org/10.1002/9783527619825.